3D Opacity Profile and Model Transmission Spectra for Extrasolar Planet Atmospheres

A Thesis Submitted in Partial Satisfaction
of the Requirements for the Degree of
Bachelor of Science in Physics
at the
University of California, Santa Cruz

By
Megan I. Shabram
March 6th, 2009

Jonathan J. Fortney
Technical Advisor

David P. Belanger
Supervisor of Senior Theses,
2001-2009

David P. Belanger
Chair, Department of Physics

ABSTRACT

In this study, we examine the consequence of both day and night side chemistry when calculating the slant optical depth through the atmosphere of a transiting extrasolar gas giant, in particular HD189733b. The tidally locked nature of gas giants with small orbital radii results in large day-night side temperature differences. As a consequence, the two sides of the planet have different molecular composition, hence different absorption features. In order to create an accurate opacity profile for these planets, these day-night discrepancies need to be accounted for. Here, the slant optical depth is calculated as a function of wavelength for various heights on a radius grid, superposed with a set of synchronous pressure-temperature profiles and corresponding molecular cross sections at various latitude and longitude points. When examining the planet radius as a function of wavelength, we find absorption features that represent both day and night side chemistry simultaneously. This can be observed with the Hubble and Spitzer space telescopes. This process yields a more accurate characterization of the opacity profile and transmission spectra for different extrasolar gas giants of current research interest.

Table of Contents

INTRODUCTION

For years it seemed that there was only one plausible explanation for the semi-controversial subject of whether or not we are alone in the universe. A few years ago, I realized for the first time how vast the universe really is, while watching old recordings of Carl Sagan's *Cosmos*. It seemed asinine to think that the happenings on Earth were a one-and-only occurrence. As I progressed through my undergraduate career in astrophysics, I came to realize that there is really only one way to address this question of whether or not there is life beyond our planet, and I best get involved. Contributions to this area of research are critical for future generations and ongoing efforts in an attempt to make groundbreaking extrasolar discoveries, whatever they may be.

Within the last 25 years, researchers have expanded the search for life beyond our solar system, finding other star-planet systems. At this time, 342 extrasolar planets have been discovered, 58 of which transit there parent star,[1] through the use of numerous methods of detection. The radial velocity detection technique[2] has proven very successful, especially in providing researchers with candidates for transiting[3] extrasolar planets. The partial occultation of a star by a planet provides a wealth of information. If an extrasolar planet's orbital plane is parallel to the line-of-sight from earth, i.e. the orbital plane is viewed approximately edge-on, then the planet can be observed passing in front of its parent star and a drop in the star's luminosity can be detected. Graphically, this is represented by a light curve - a plot of the star's intensity versus time as the planet traverses across it (see Fig. 20). Using the information from the light curve coupled with the radial velocity data, and with a reasonable approximation of the stellar mass, the extrasolar planet's orbital inclination, period, mass, and radius can be inferred[4] (de Pater and Lissauer 2001). In addition, information about the planet's atmosphere can be obtained observationally and compared to theoretical models. Instruments such as the Space Telescope Imaging Spectrograph (STIS) onboard the *Hubble Space Telescope*

[1] For an up-to-date list visit www.exoplanet.eu.
[2] A more in depth explanation of the radial velocity detection method can be found in appendix A.
[3] See Glossary for any terms that are unfamiliar throughout text.
[4] For radial velocity equation, refer to appendix B.

(HST) and the Infrared Array Camera (IRAC) onboard the Spitzer Space Telescope (SST) make extrasolar planet atmospheric transmission spectra available for analysis.

During a transit, these instruments see the planet's absorption spectrum superimposed on the stellar spectrum (J. J. Fortney 2005, and references therein). When modeling a transit, the planet can be interpreted as an opaque disk with an annulus of transparent atmosphere through which the parent star's light passes through (see Fig. 4). The detected absorption features can give researchers information about the atmospheric structure and composition. Observations are limited to cases where the planet-to-star radius ratio[5] is large and the atmosphere is very hot, puffed up, with a large scale height, so that the latest instrumentation is able to detect it. As a result of these constraints, researchers are focused on producing atmospheric models for a genre of planet: gas giants with a small semi major axis and a mass on the order of Jupiter's. These planets are sometimes referred to as "hot Jupiters". More recently, a cooler class of planets known as hot Neptunes are breaking into the field, as well as the discovery of super Earths, planets on the order of 1-10 Earth masses. Current models also assume a parent star with a solar composition similar to the Sun's when incorporating atmospheric chemistry. Solar abundances and meteoritic CI chondrite abundances are constantly updated and are at researcher fingertips, whereas chemical abundances in distant star-planet systems are of greater uncertainty. These abundances are used to compute condensation temperatures for the elements (Lodders 2003) and give insight into an atmospheric molecular composition that is very temperature and pressure sensitive. The composition of early stage meteorites as well as stellar composition supplies information about the planetary nebula and in turn, the constituents of the planets that formed.

As opposed to what one might expect, a hot Jupiter is relatively different from the Jovian planets of our solar system. The close proximity of these gas giants to their parent star lead to tidally locked orbits as well as higher temperatures (Knutson, et al. 2007). For HD189733b, temperatures range from around 300K on the night hemispheres, up to around 2000K in the hot dayside regions of the planet. This ultimately affects the molecular composition of the atmosphere, and therefore alters the absorption features. For instance, carbon chemistry is very sensitive to temperature, resulting in a CH_4

[5] In our solar system $R_{Jupter}/R_{Sun} \sim 0.1$

dominance in carbon based molecules for cooler gas giants such as Jupiter and CO dominance for the warmest hot Jupiters (Marley, et al. 2006). CH_4 absorbs wavelengths at of 1.4, 1.7, and 2.2 μm, while CO absorbs at wavelengths of 1.2, 1.6, and 2.3 μm (Hubbard, et al. 2001), hence contributing to a difference in absorption spectra.

One highly studied extrasolar giant planet, HD189733b, is close-in and presumably tidally locked, meeting the standard qualifications previously mentioned for acquiring a quality atmospheric spectrum, and it is also around a bright parent star. HD189733b has a short 2.2-day period, implying that it must be heavily irradiated, yet its parent star is relatively cool resulting in HD189733b being classified as a pL type planet. A pL type planet is relatively cooler, with more evenly distributed atmospheric conditions where pM type planets are hotter with dynamical time scales longer then radiative time scales, thus reducing the distribution of energy throughout the atmosphere (Fortney, et al. 2008). HD189733b orbits a spectral type KI to K2 star, meaning that the star is extremely massive and luminous yet its temperatures are on the order of 3,500-5,000K; cool enough for simple molecules to form[6], therefore influencing its emission spectra. The mass of this gas giant has been determined to be $1.13\pm0.03M_J$, its radius $1.138\pm0.027R_J$, its orbital inclination 85.76 ± 0.29^0, and located at a right ascension 20 00 43 and declination +22 42 39[1]. Transmission spectra for this planet's atmosphere were obtained by Swain et al. (2008) in the near infrared, Tinetti et al. (2008) in the infrared, and Pont et al. (2008) in the optical.

As a consequence of the tidally locked nature of hot Jupiters such as HD189733b, a day-night temperature gradient is induced. With this in mind, the atmospheric chemistry also varies on either side of the terminator. In order to accurately model transmission spectra of a hot Jupiter atmosphere, the resultant chemical gradients need to be considered. Here we present a method to realistically model transmission spectra with attention to these atmospheric variations.

[6] See http://www.glyphweb.com/esky/concepts/spectralclassification.html.

ANALYSIS

When modeling an extrasolar planet atmosphere, many factors are involved. The temperature and pressure profile of the planet needs to be understood as well as the molecules that are capable of existing at these pressure-temperature (P-T) values. The radial dimension of the atmosphere is also subject to variations in the pressure, temperature and molecular composition. In this model, we interpolate a pressure-temperature profile with corresponding absorption coefficients onto a radius grid, and calculate the slant optical depth through the atmosphere for approximately one thousand radial points. We execute this process for a range of wavelengths, obtaining model atmosphere transmission spectra. We later expand the model from one dimension to three dimensions, incorporating pressure-temperature profiles characteristic of different regions on the planet, which is further discussed in section 3, *Evolution of the Model*.

1. OPACITY AND OPTICAL DEPTH

Starting at the beginning, we know right away that certain materials are absorbent in some wavelengths, yet transparent to others. Consider isolating a material made of one molecule. Next, take this material and shine one wavelength of light onto it. That particular wavelength will either be absorbed, scattered, or pass through the material, depending on its molecular structure. If the wavelength gets absorbed or scattered, the material is deemed to be opaque to that wavelength, and if it passes through with ease, it is transparent. Examining how this material behaves for a range of wavelengths constitutes an opacity profile for that material. This process is modeled for extrasolar planet atmospheres, which are composed of a variety of molecules, each present in different regions of the atmosphere depending on the associated P-T profile.

When a beam of light with a particular frequency passes through a medium, its characteristic intensity can be reduced. Lambert's exponential absorption law defines the observed intensity as

$$I_\nu(\tau_\nu) = I_\nu(0)e^{-\tau_\nu} \tag{1}$$

where $I(\tau_v)$ is the observed intensity, $I(0)$ is the initial intensity, and τ_v is the optical depth of light with a frequency v through the medium (de Pater and Lissauer 2001). The optical depth is a dimensionless quantity representing how much light is removed by scattering or absorption as it passes through a medium. The optical depth through a propagation length ***s*** is expressed as

$$\tau_v(s,s') = \int_s^{s'} (k_v \rho) ds \tag{2}$$

where τ_v is the optical depth, k_v is the absorption coefficient (units are usually cm^2/g), and ρ is the mass density (Chamberlain and Hunten 1987). Understanding the optical depth is important in the process of finding out how a medium reacts to different frequencies of light and in turn, its chemical structure.

During an extrasolar planet transit, the observed transmission spectra are from stellar light passing through the atmosphere tangential to the planet surface. The optical depth of interest is called the slant optical depth. In familiar terms, the slant optical depth on Earth would be the amount of light that makes it to an observer as they look across the planet's surface towards the horizon. The normal optical depth is represented by the path an observer sees when looking straight up into the sky, normal to Earth's surface (see Fig. 1)

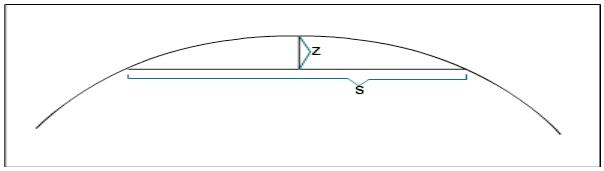

Figure 1. Slant optical depth versus normal optical depth through atmosphere. Here, *s* is the direction through the atmosphere at which the slant optical depth is calculated whereas *z* represents the normal optical depth propagation direction.

The slant optical depth through an extrasolar planet atmosphere is used to model transmission spectra. It is possible that condensate hazes are present among the gaseous absorbers in these hot Jupiter atmospheres. These hazes present complications when characterizing atmospheres using transmission spectroscopy as they can result in a slant

optical depth of approximately 35 to 90 times the normal optical depth (J. J. Fortney 2005). These condensates may block gaseous absorption features that would otherwise be present for normal viewing geometry (Pont, et al. 2007).

2. METHOD

In order to model the slant optical depth through the atmosphere of an extrasolar planet for a given wavelength, we need to first know what possible molecules could exist in the atmosphere of interest, and at what P-T points they are present for. Our model does this by reading in a table of absorption coefficients for prospective P-T points. The absorption coefficients essentially represent the amount of area a particular molecule will take up in the medium, i.e. the cross section of a particular molecule. The absorption coefficients are obtained from laboratory or computational studies of individual molecules or atoms (Freedman, Marley and Lodders 2008) and the relative abundances of chemical species at particular P-T points through Gibbs free energy (Lodders and Fegley 2006). Gaseous absorbers present in extrasolar gas giants are H_2, H_2O, CH_4, CO, and alkali metals, mainly Na and K.

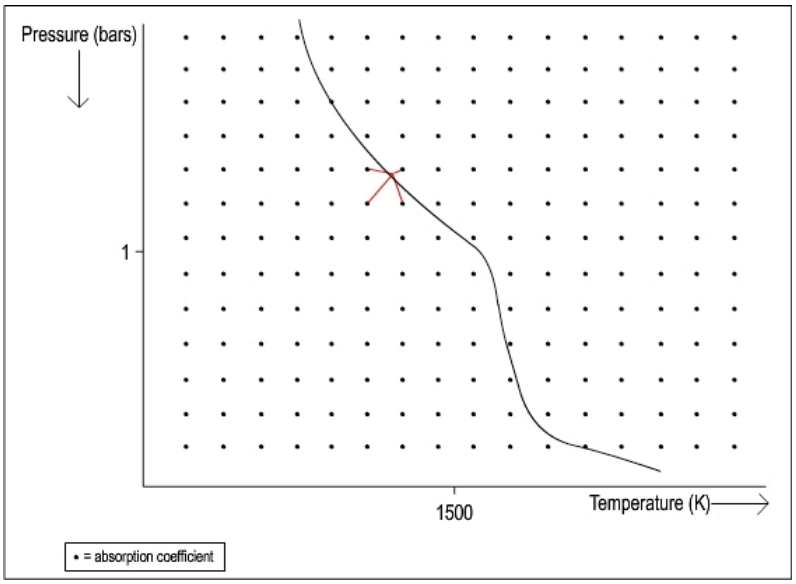

Figure 2. Absorption coefficient grid with overlying P-T profile. There are absorption coefficients for a number of pressures and corresponding temperatures. The P-T profile of interest looks through the table and averages the four closest absorption coefficient values at each point of interest along the curve.

A P-T profile is then overlaid on the pressure, temperature, and wavelength dependent absorption coefficient table. The absorption coefficients for the model atmosphere (units are cm^2/particle) are then determined for each P-T point by averaging the closest four values on the table that coincide with the overlaid pressure-temperature curve (see Fig. 2). We then use these absorption coefficients to represent the molecular cross section for regions in the atmosphere, also adding cross sections resulting from Rayleigh scattering. It is to be noted that we include methane abundance information separately from the absorption coefficient table. This is because the behavior of methane in extrasolar planet atmospheres is poorly understood, laboratory analysis of the methane spectrum is incomplete, and laboratory measurements alone are not enough to complete it (Freedman, Marley and Lodders 2008). After these steps have been taken, we have acquired a grid of temperatures, their associated pressures, and the corresponding molecular cross sections, ready to be used in an optical depth calculation.

Before we are able to calculate the slant optical depth, we need to obtain the density of the medium (see equation 2). The gaseous nature of the atmosphere permits us to implement the ideal gas law,

$$PV = k_B T, \tag{3}$$

where P is pressure, V is volume, k_B is the Stephen-Boltzmann constant, and T is the temperature. From this we can calculate the density, or particle per volume (cm^3),

$$\rho_j \cong \frac{\text{particle}}{V} = \frac{P}{k_B T} \tag{4}$$

where the pressure and temperature are characteristic of the altitude in the atmosphere that the slant optical depth is to be calculated for. Putting this together with the Rayleigh scattering plus the gaseous and alkali opacity cross-section, σ_λ, and the propagation length, Δs, and summing over the total length, or the total distance the light has to travel through the atmosphere, we obtain a formula for numerically integrating the slant optical depth (see Fig. 3):

$$\tau_\lambda = \sum_1^i \sigma_{\lambda,i}\rho_j(\Delta s). \tag{5}$$

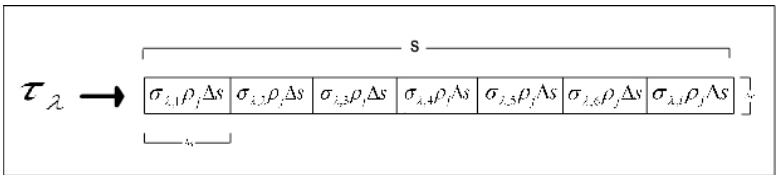

Figure 3. Numerical integration of slant optical depth. Each box represents the optical depth through a propagation length ***Δs***. All boxes are summed to obtain the optical depth through a total propagation length ***s***.

The slant optical depth is needed for a range of altitudes in the atmosphere so we interpolate the P-T profile of interest onto ~1000 point radius grid, using initial values for the assumed surface radius of the planet, along with the surface gravity and surface pressure. These values are 85,790 km, 21ms^{-2}, and 1bar respectively for the planet HD189733b.

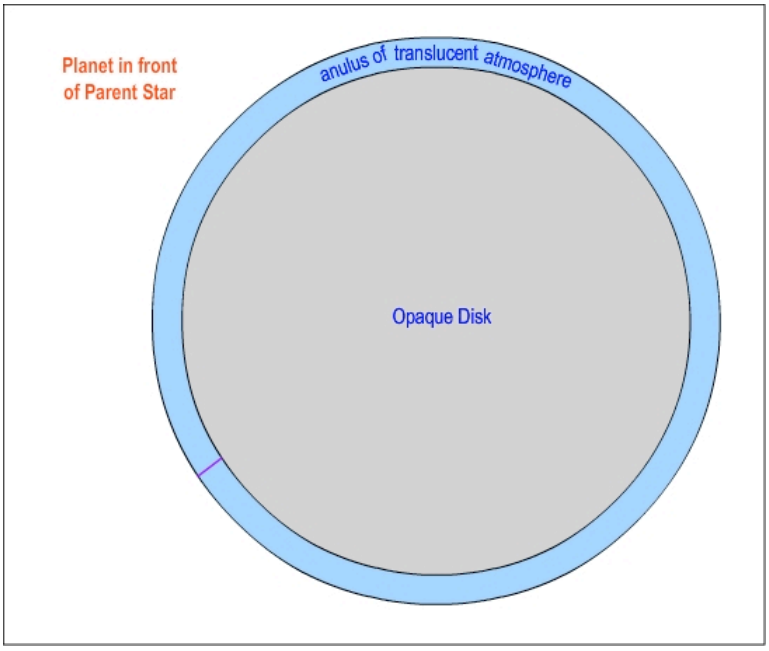

Figure 4. Observer's view of transiting planet. Opaque region of the disk blocks out stellar light from the observer. Light can pass tangentially through annulus of transparent atmosphere and absorption features can be observed and theoretically modeled. The planet disk resembles a cross section through the terminator of the planet.

For each step up in the atmosphere, the pressure is calculated, hydrostatic equilibrium is assumed, and the matching temperature from the P-T profile is also assigned to that step. This process yields one thousand values for the radial distance from the planets surface, each with an associated temperature and pressure, along with an associated molecular cross section.

Getting to the heart of things, when the planet transits its host star, the planet is depicted as an opaque disk surrounded by an annulus of transparent atmosphere (see Fig. 4), from which spectra can be obtained. The spectrum is produced by light passing tangentially through the atmosphere of the planet. This light has to travel further through the atmosphere the closer it is to the planet's "1 bar surface" as a result of the slant geometry and the spherical nature of the planet. The opaque center of the planet, or the opaque disk, blocks stellar light that would otherwise pass through the atmosphere in the front and back of the planet, from an observer's point of view. The instruments are only able to see light passing through a portion of the planets atmosphere. This portion bears a strong resemblance to a round bead that has an oversized cylindrical hole. When finding the length through the atmosphere that the light has to travel at a particular radius, we model the tangential distance through a slice out of the side of the bead-looking atmosphere, where the slice resembles a semi-circle (see Fig. 5).

The first step in creating the slice of atmosphere is to construct it using a grid. We do this by dividing the height of the atmosphere by one thousand, to represent each radius point, and call this Δr (see Fig. 6). We then find the length of half the bottom of the slice (half of the longest part of the slice) and divide that by one thousand, calling this Δs (Note: Δs will be much greater then Δr). We then match the radius grid (and corresponding pressures, temperatures, and cross-sections) to the radial part of the grid we created that represents half of the slice. Each radius value is distinguished by assigning it a number one through one thousand, and referring to it as $r(j)$, where $r(1)$ is the radius of the top of the atmosphere and $r(1000)$ is the radius at the bottom. Using this setup, we construct one side of the slice. The area of the slice at the top of the atmosphere, at a height $r(1)$, is a box of Δr by Δs. Stepping down in the atmosphere to a height of $r(2)$ another box is added, so the area of this strip of atmosphere is now Δr by Δs plus Δr by Δs (two boxes summed).

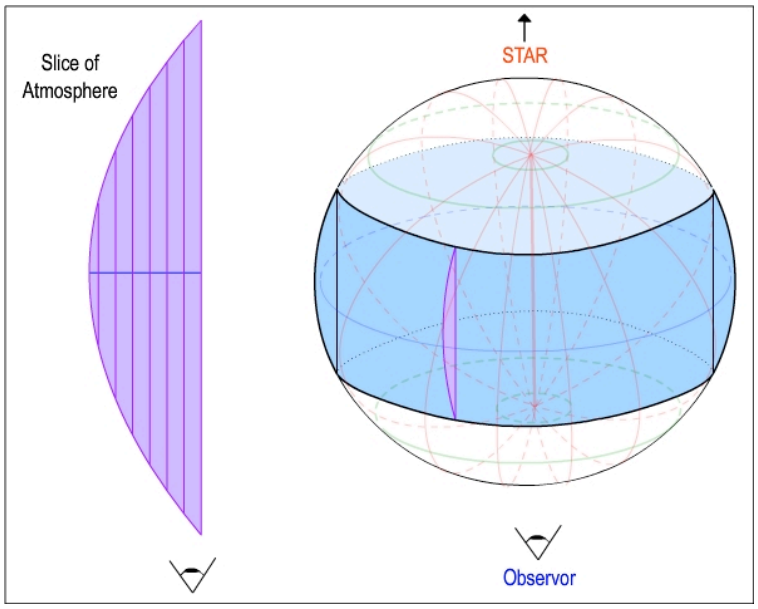

Figure 5. Portion of atmosphere observed and modeled. This is a geometrical representation of the portion of the atmosphere that allows stellar light to pass through. It resembles a spherical bead with at large cylindrical hole, as a result of the opaque region blocking the passage of light. The purple semi-circle is a slice out of the atmosphere that the slant optical depth is modeled for. The vertical lines across the slice represent the propagation direction. The blue perpendicular line on the slice represents the terminator of the planet.

For each step down in the atmosphere, an additional box is added so $r(3)$ would be the sum of three boxes. At the bottom of the atmosphere the radius is $r(1000)$ and the area of the strip is one thousand of the boxes added up. Stacking up each of these strips, a half semi-circle starts to form. To create the entire half circle or slice of atmosphere, each strip of the grid is then doubled, and there will be twice as many boxes in each row of atmosphere (at $r(1000)$ there will be two thousand boxes). If you were wondering why the density in equation (5) has a subscript ***j***, it is because the density will be a function of the temperature and pressure values for each height ***r*** as a function of ***j***. The slant optical depth equation is thus

$$\tau_{\lambda,j} = \sum_{i=1}^{j} \sigma_{\lambda,j}(i)\rho_j(i)\Delta s, \tag{6}$$

where the optical depth is calculated for each box and summed over i for each radius point (see Fig. 6). Note that the optical depth calculation is independent of Δr. The distance through the medium, Δs, is the length of interest in the calculation, and we assign a slant optical depth for a portion of the height, Δr, in the atmosphere.

Once the slant optical depth is obtained as a function of altitude for a range of wavelengths, also known as an opacity profile, we are ready to build a transmission spectra. A slant optical depth of 0.56 has been shown to represent the edge of the planet (Lecavelier des Etangs, et al. 2008). With this information we examine the radial slant optical depth values, and for a particular wavelength, we find the altitude in the atmosphere that corresponds to this edge optical depth value. Adding this atmospheric height with the surface radius of the planet gives us an effective planet radius for a particular wavelength. Repeating this process for a range of wavelengths we obtain the effective planet radius as a function of wavelength, this is also known as a transmission spectrum.

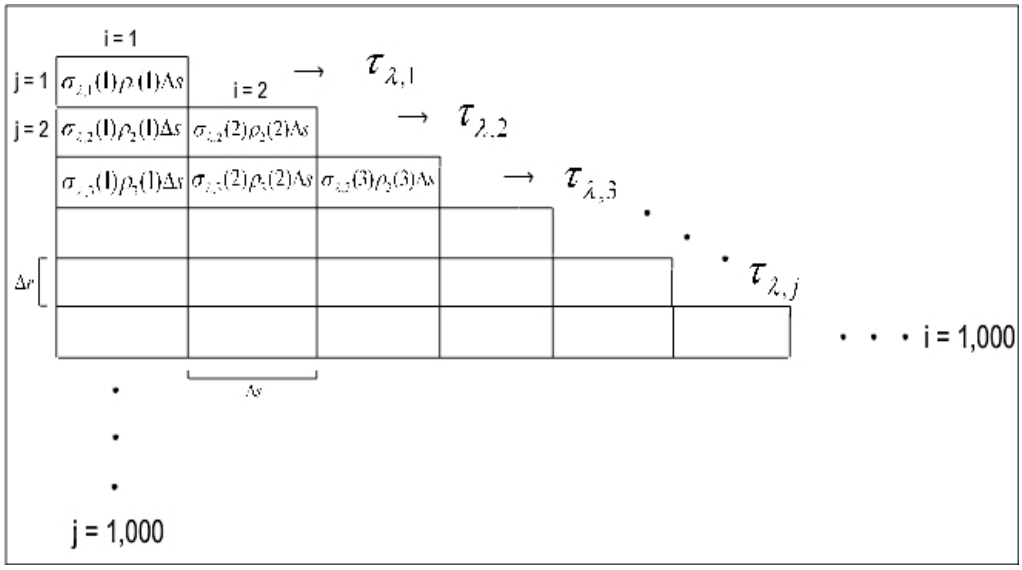

Figure 6. Slant optical depth integration for radial points of atmospheric slice and associated propagation lengths. For each step down in the atmosphere, another section is added to the slant optical depth summation. This width is much larger than the height of each box, tracing out half the slice of atmosphere. Each strip for the radial heights in the atmosphere are doubled in order to produce the slant optical depth through the entire slice. This one-dimensional model assumes a globally uniform atmosphere.

3. EVOLUTION OF THE MODEL

The latest transmission spectra are modeled using atmospheric opacity profiles that assume a uniform atmosphere, using one P-T profile expected to represent the entire planet. In reality, the temperature, pressure and in turn composition will vary in different regions, especially from the day to night sides of these synchronously orbiting gas giants. The substellar point of the planet's atmosphere is the point in the atmosphere that is directly in front of the star. This would seem to be the hottest place in the atmosphere, yet it has been shown that dynamical processes result in the hot spot of HD189733b to be shifted 16 ± 6^0 east of the substellar point due to winds. The incident stellar energy is distributed and transported with modest efficiency to the night side hemisphere (Knutson, et al. 2007), and the equatorial jet being a good mechanism for this process (see Fig. 10). The equatorial jet is a hot wind driven region flowing around the planet's equator.

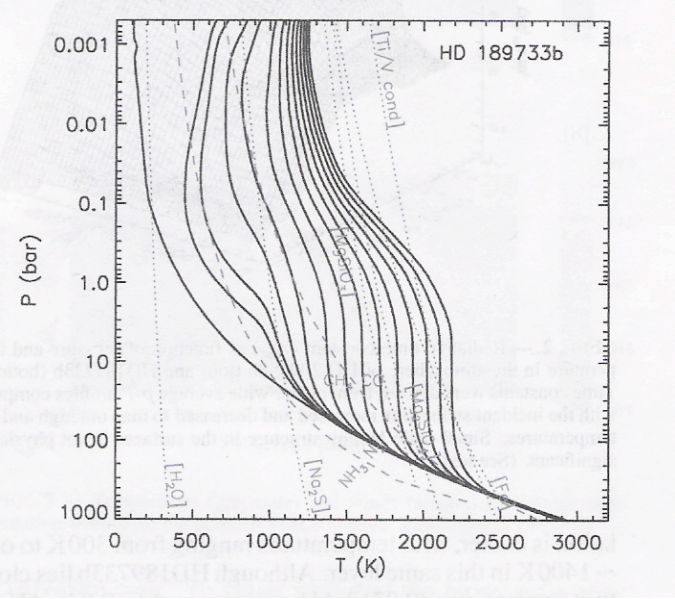

Figure 7. Regionally specific Pressure-Temperature profiles. Each P-T line represents a profile for the dayside atmosphere of HD189733b. The hottest profile corresponds to the substellar point in the atmosphere, and the cooler profiles represent the concentric circular regions of atmosphere as you move away from the substellar point, the coolest profile representing the terminator (Showman, Cooper, et al. 2008). Note: this is a simple model that does not consider winds.

Even with this in mind, it is still true that an atmospheric location closer to the substellar point experiences deeper penetration of stellar flux creating a warmer region with more absorption, and for locations closer to the terminator of the planet, the opposite is true (Showman, Cooper, et al. 2008). The P-T profiles are also subject to variations resulting from this phenomenon. Figure 7 shows P-T profiles for the dayside of HD189733b; the hotter profiles represent the region of the atmosphere closer to the substellar point and the cooler profiles represent atmospheric conditions near the terminator. When calculating the slant optical depth through a slice of a transiting planet's 3D atmosphere, a method for tracking the location and its associated temperature-pressure

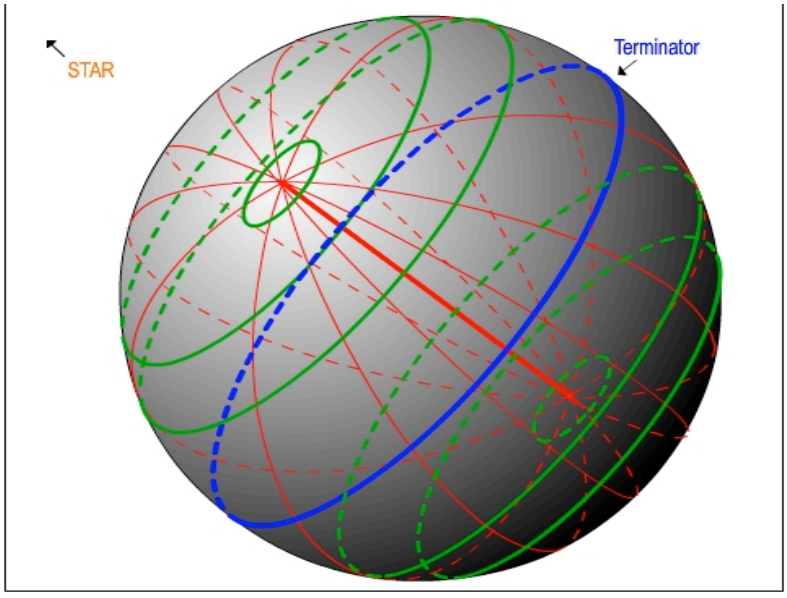

Figure 8. Rotated coordinate system for pressure-temperature profile location. The axis of the longitude and latitude coordinate system is now the axis of the opaque region of the planet model. This allows for a cleaner slant optical depth numerical integration around the terminator.

profile needs to be put into action. To do this, we assign a longitude and latitude point to each profile. It is to be noted that a coordinate system of this type is conventionally aligned with the rotation axis, as in the Earth's standard latitude longitude grid, meaning,

the longitudes come together at either end of the axis of rotation. For our purposes, this has the unfortunate draw back that paths through the atmosphere near the poles have a much higher density of longitude and latitude points than paths near the equator. To avoid this issue and to ease our calculation, we rotate this coordinate system 90^0 so that it corresponds to the axis of the opaque cylindrical region of the model (see Fig. 8) and the north pole moves to the planets substellar point. In doing this, we preserve the uniformity of the temperature-pressure profile coordinate locations around the terminator of the planet, allowing for a cleaner integration calculation. The calculations become simplified because we can now just follow a "longitude" when following a path from day to night (see Fig. 9).

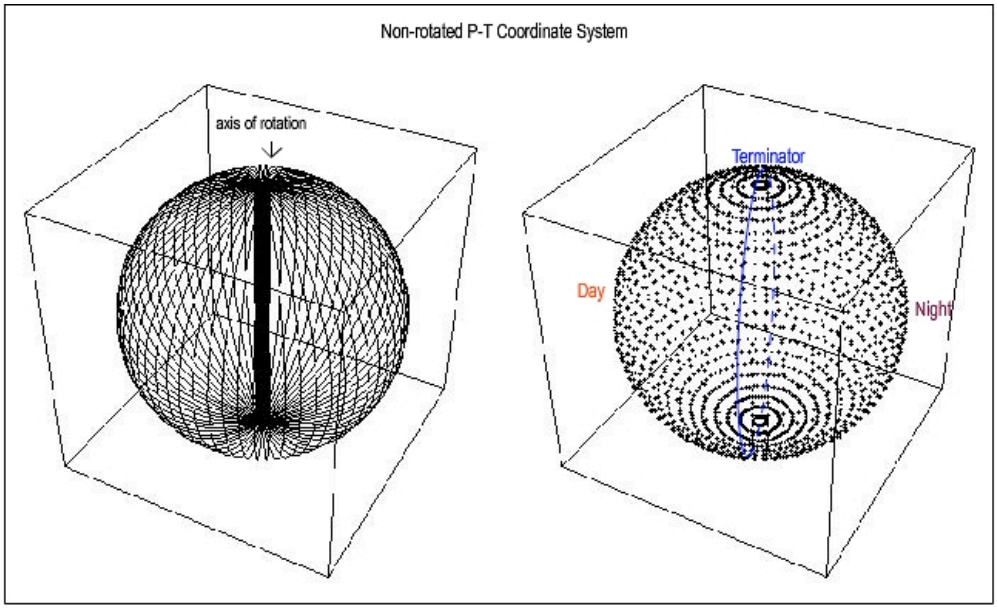

Figure 9. Non-rotated coordinate system. Using the non-rotated coordinate system, there will be a larger flux of longitude points around the poles of the planet and in turn the terminator. This complicates how we calculate the slant optical depth through the atmosphere above the limb, or outer edge, of the opaque section of the planet. (courtesy: P. Shabram).

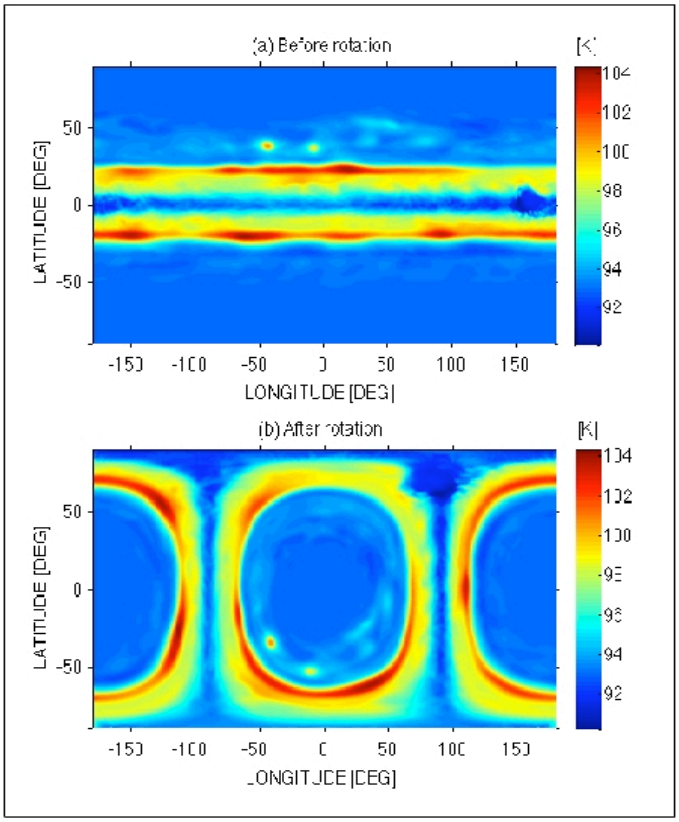

Figure 10. Temperature field for rotated and non-rotated coordinate system. This is a temperature field at 0.2 bars for Saturn, a gas giant in our solar system. It is the same field, but with different coordinate representation. (courtesy: Y Lian)

We are particularly interested in modeling the region of the atmosphere near the terminator because it is a combination of both day and night side conditions and it is the region probed during the transit. Furthermore, an example of the same temperature field of a gas giant before and after rotation looks very different (see Fig. 10) as the equatorial jet is still wrapped around the equator of the planet, yet is in the same plane as the coordinate system axis after rotation. Using this coordinate orientation, we can see that each longitude will represent a strip, or one slice out of the side of the 'bead' (see Fig. 5) and each latitude point for a particular longitude will create an angle with respect to the terminator of the planet (see Fig. 11).

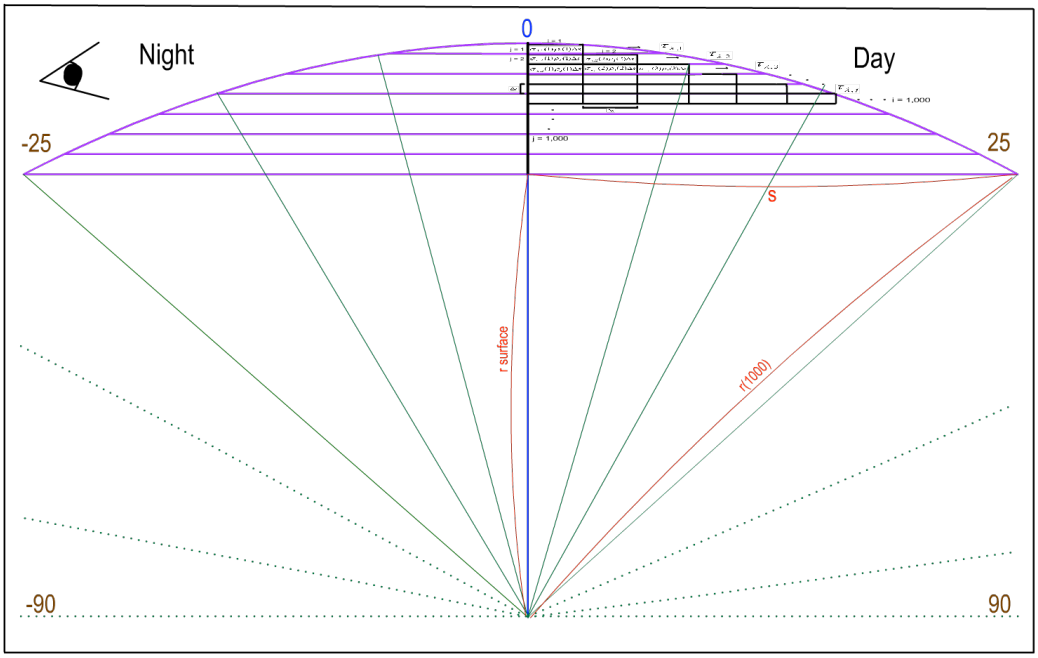

Figure 11. Representation of the angular dependence for the slant optical depth calculation for a given longitude. Each green line separates out a portion of the slice. For that portion, a regionally specific P-T profile is used to obtain the absorption coefficients and the molecular densities used in the calculation. This will provide a more realistic model that will take into consideration both day and night side chemistry. Only latitudes within 25^0 of the terminator are calculated.

When the slant optical depth is being numerically integrated in the 2D model, it fills in the optical depth grid for the angular region of the slice corresponding to the P-T profile designated to that angular coordinate. The latitude location of each P-T profile on the planet serves to separate regions of the atmosphere slice that have different structures. As it cycles through each latitude point, the grid eventually is completely filled in. On that account, the slant optical depth for each box comprising the slice is unique to its region in the atmosphere and the corresponding P-T profile[7]. After repeating this process for a range of longitudes around the planet, we have a three-dimensional opacity profile from which a three-dimensional transmission spectrum is acquired (see Fig. 12).

[7] See appendix C for an explanation of this portion of the computer model.

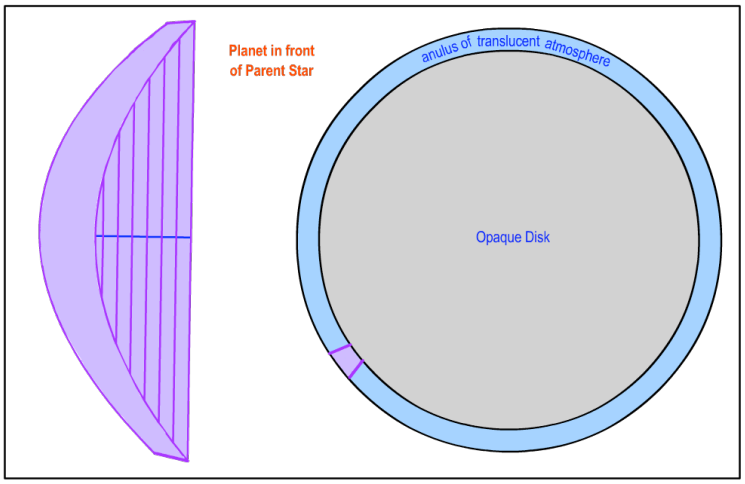

Figure 12. 3D model produces transmission spectra for entire ring of atmosphere. The slice shown in this figure represents a region between two longitude strips for which the calculation is made.

RESULTS

Transmission spectra are a good means of characterizing an extrasolar planet's atmosphere because they provide a wavelength dependant planet radius which is a reflection of the opaqueness of the planet to a particular wavelength resulting from molecular absorption and scattering: the more opaque the planet appears to a particular wavelength, the larger the planet radius. The opaqueness, and in turn the effective radius of the planet, depends on the pressure and temperature structure of the atmosphere. With this in mind we can see how transmission spectra might look as you vary certain parameters. When modeling 1D isothermal transmission spectra of HD189733b, we can examine the absorption features of models using a constant temperature profile and extrapolate what might be occurring on hotter versus cooler planets as well as hot or cool regions of a planet (see Fig. 13). Evaluating the effects of a constant temperature profile at optical wavelengths, we see that colder planets exhibit sodium (Na) and potassium (K) absorption spikes at the 589nm and 770nm wavelength points. As the temperature is cranked up we see the atmosphere become more puffed up as the gases are expanded, meaning the scale height increases, and we see more band-like absorption features that

likely result from titanium oxide (TiO) and vanadium oxide (VO) gasses, in the .3-1 μm band, that can exist in the upper atmosphere of the planet at these high temperatures.

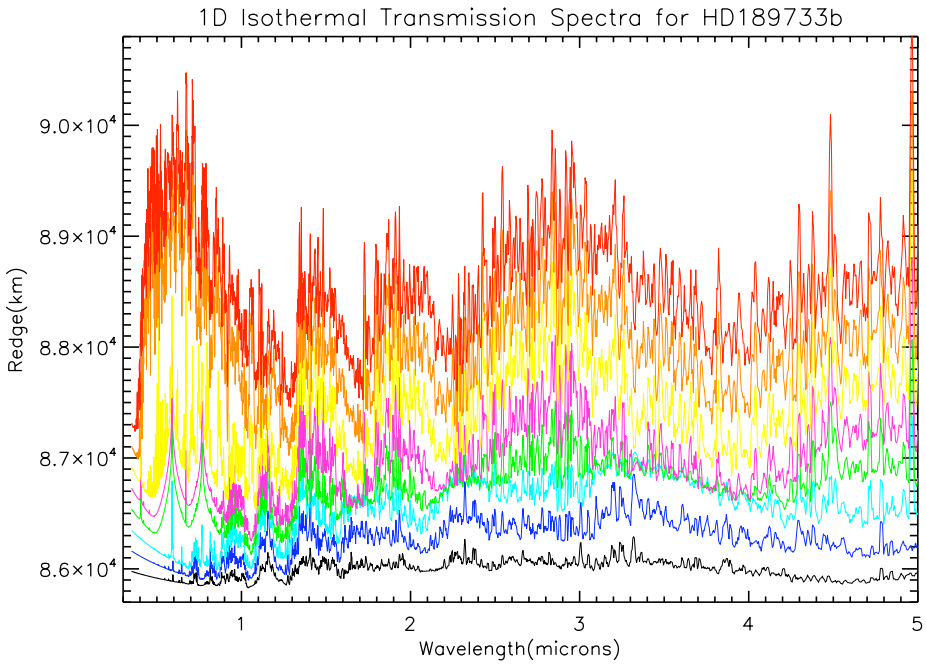

Figure 13. Isothermal 1D models for HD189733b. Variations in absorption features can be seen here, as the temperature is varied. This can tell us about the atmospheric conditions and molecular composition of the hot versus cool planets as well as hot versus cool regions of the atmosphere. Temperatures are 250K for the black curve, 500K, 750K, 1000K, 1250K, 1500K, 1750K, up to the red curve of 2000K.

At low temperatures the TiO and VO condense out, revealing the presence of the Na and K alkali absorbers. The TiO and VO serve to mask the sodium and potassium spikes as the atmosphere is heated. Note that the dayside atmosphere can become depleted of neutral Na, K, and other species via ionization (Sing, et al. 2008), but this effect is not incorporated into the model. For the coldest models, in the optical, Na and K are lost to clouds, and CH_4 bands are seen instead. Planets that are cooler (as would happen further from a parent star) with short atmospheres will result in transmission spectra that appear more smashed or span a smaller radius range. Figure 13 shows this effect as well, where the colder temperature transmission spectra span a smaller radius range and show a more

condensed atmosphere. Again, we consider this a 1D model because it is obtained using one pressure-temperature profile that is suppose to represent the entire planet.

When applying a 2D modeling method using regionally specific pressure-temperature profiles for HD189733b, the results should agree with the 1D isothermal model.

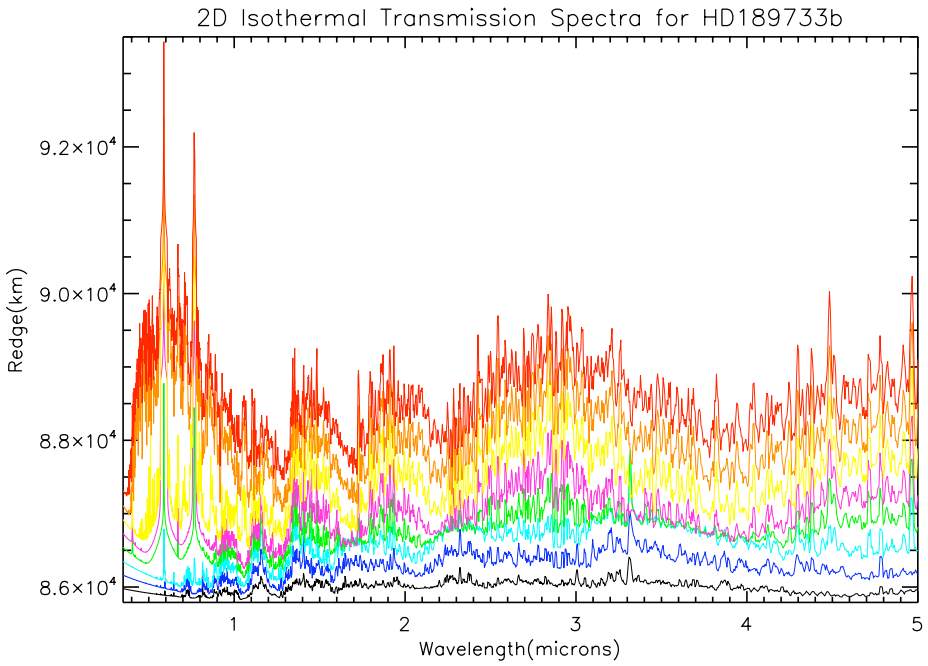

Figure 14. 2D isothermal transmission spectra of -180 longitude strip.

The isothermal models use a profile that pairs all the pressure points with a constant temperature value when performing the calculations. Comparing the 2D isothermal model to the 1D isothermal model of HD189733b, we can see a difference in the .35-1 μm range. The 2D model shows more extended Na and K lines. This has yet to be explained, and is under investigation.

We effectively extend the model to 3D by modeling 2D strips of atmosphere at different longitudes (of the rotated coordinate system) around the planet. Figure 15 is the temperature field used in the 3D model. The top panel is at the 1mbar atmosphere level, the middle panel is for the 30mbar level, and the bottom panel is at the 1bar level.

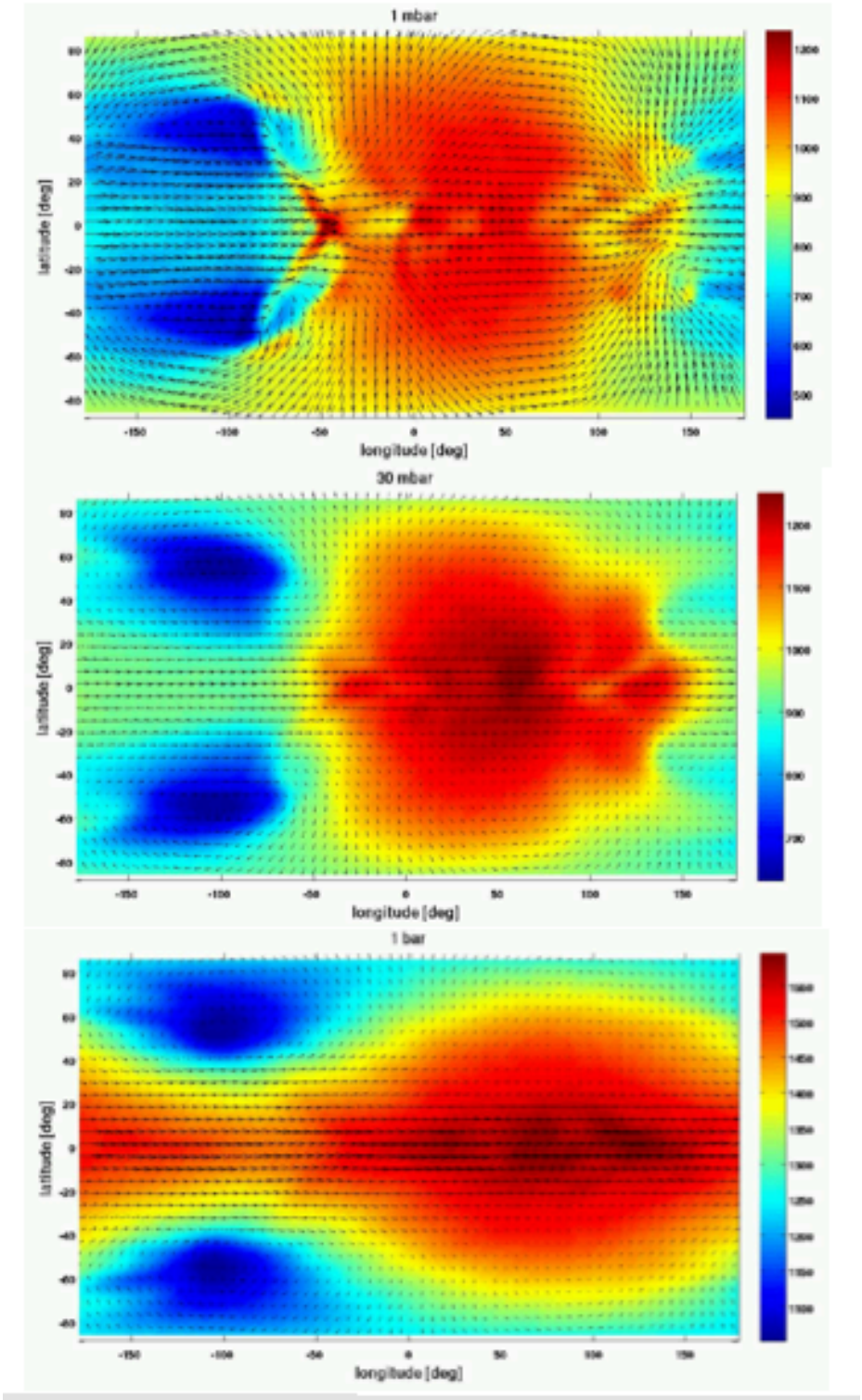

Figure 15. 3D temperature field for HD189733b. Here the temperature scale is in K, and the arrows represent the winds. The resolution is 128 x 64 longitudes and latitudes with 40 vertical layers. In this figure the substellar point is at longitude and latitude of 0^0, and 0^0, which is for the non-rotated grid (Showman, Fortney, et al. 2007).

Figure 16 is a 3D transmission spectra model, consisting of an average of 8 transmission spectra for longitude strips around the planet (see Appendix D for a separate plot of each of the 2D transmission spectra used in the average).

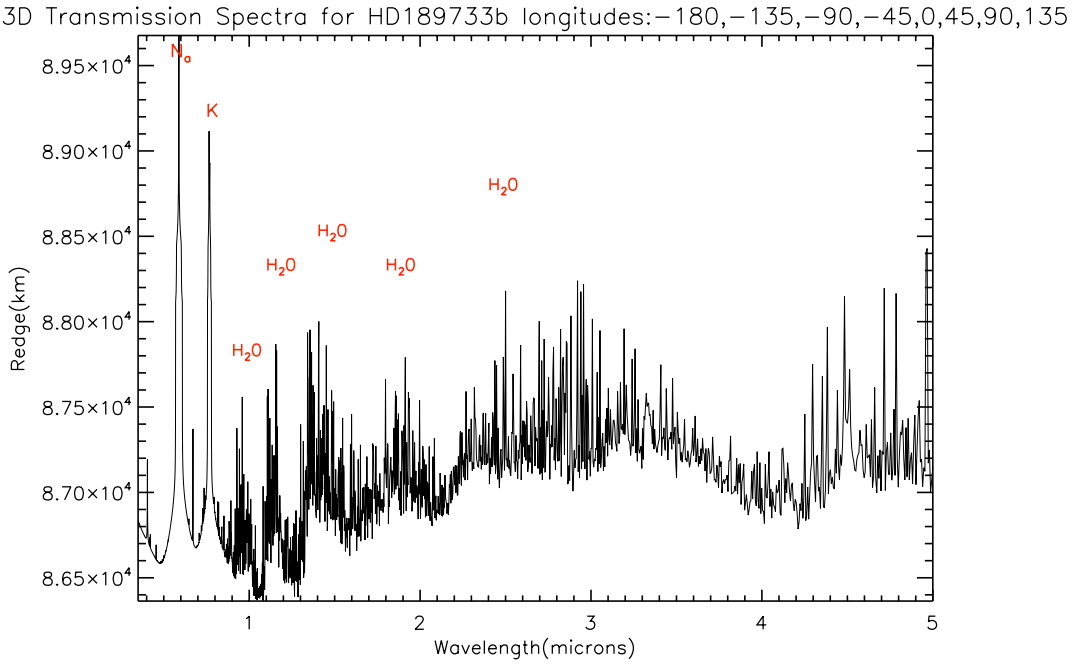

Figure 16. 3D transmission spectra using 8 longitude strips around planet. This 3D model is an average of longitude atmosphere strips for -180^0, -135^0, -90^0, -45^0, 0^0, 45^0, 90^0, and 135^0. Each separate curve can be found in appendix D.

The dominating features present in these transmission spectra are absorption from neutral Na and K, and absorption due to gaseous species such as H_2O are present.

The atmosphere of HD189733b has complicated atmospheric dynamics, containing a hot equatorial jet spanning 30^{0}N to 30^{0}S in the original coordinate system (Showman, Fortney, et al. 2007). This is equivalent to the 60^0 to 120^0 longitude range of our rotated coordinate system. When comparing the 90^0 longitude strip that lies within the region of the equatorial jet, to the 180^0 longitude strip that goes across the north pole of the planet, we see hot versus cold transmission spectral features (see Fig. 17). The colder region of the planet produces transmission spectra that show smaller planet radii for the same wavelengths as the hotter region. We can also see features in the 2 to 5 μm range that suggest there are different absorbers in the hot region of the planet compared the cooler

region of the planet for these wavelengths. This could possibly result from CO and CH_4. In the hot region (red curve) we can see stronger absorption in the 2.2 and 4.7 μm lines possibly resulting from the dominant carbon based absorber being CO. In the colder region (blue curve), we see a peak in absorption at the 2.2 and 3.3 μm line, possibly resulting from a methane dominant region in the atmosphere.

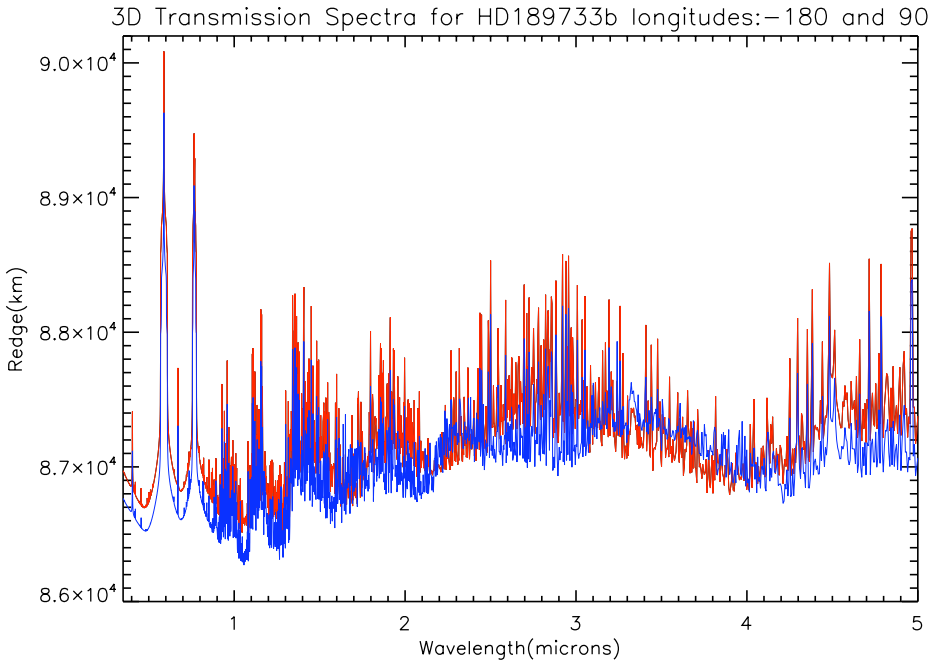

Figure 17. Hot versus cold 2D transmission spectra. The red curve is a 2D plot of transmission spectra through the east side of the equatorial jet of the planet at a rotated longitude of 90^0, while blue curve is for a colder region of the atmosphere at a rotated longitude of -180^0 going through the real north pole of the planet.

With a closer look at the 3D model, it can be seen that transmission spectra through the east side of the planet, specifically, the region between the 45^0 and 135^0 longitudes, exhibit absorption features characteristic of hotter temperatures. The transmission spectra through 0^0, -45^0, -90^0, -135^0, and -180^0, all exhibit features characteristic of cooler atmospheric regions. This indicates that the 3D transmission spectra model is an effective method for obtaining regionally specific transmission spectra of a more realistic nature.

DISCUSSION

The 3D modeling method provides transmission spectra that are characteristic of the planet as a whole, incorporating global variations in atmospheric dynamics and composition. The small portion of atmosphere that we are able to obtain spectra for encompasses the terminator and a small region around it; hence the absorption features we see are from the cooler less irradiated portion of the dayside, as well as the warmer areas of the nightside. HD189733b is orbiting a cooler host star, which allows for dynamical mixing to compete with radiative timescales, resulting in a somewhat homogenized atmospheric conditions. The region near the terminator of this planet model is relatively mixed, and our 2D transmission spectra reflect this as they show cool Na, K and CH_4 features in transmission spectra for at large region of the annulus of atmosphere we model, with the exception of a warmer region around the eastside equatorial jet.

Here we focus primarily on modeling transmission spectra for gas giant atmospheres since detection of Earth size transits has not yet occurred. Obtaining atmospheric spectra of small planets is a complicated task, but missions such as COROT and KEPLER are up and running, capable of finding planets with masses on the order of Earth. In our models, Earth mass planets will likely have very short, compressed atmospheres, difficult to see observationally without advanced instrumentation. Some super-Earth's may have retained a large hydrogen envelope, possibly able to be observed and compared to realistic transmission spectra models (Miller-Ricci, Seager and Sasselov 2009).

A more pressing future project would be to consider the effects of wind speed on 3D transmission spectra models. HD189773b and other tidally locked gas giants experience winds that are pushed from the hot substellar point eastward to colder regions of the planet. From an observer's point of view, the winds are rushing toward them, producing a blueshift in the planets east side spectrum as it transits (Spiegel, Haiman and Gaudi 2007). Incorporating wind speeds as a function of altitude and position, we could obtain how transmission spectra are Doppler shifted, creating an even more realistic model.

Transmission spectra are important because they are dense in atmospheric information. Transit spectra are the best source of information we can obtain for

extrasolar planets at this time, and being able to interpret them using models is the best way we can learn about the planets in our neighboring stellar systems. With up and coming instrumentation and creative insight, information about these planets is growing and models are reaching levels of higher precision. With this in mind, more interesting phenomena are bound to be uncovered.

ACKNOWLEDGEMENTS

I'd like to acknowledge Jonathan Fortney, my technical advisor for providing me with interesting research, expanding my extrasolar planet knowledge and greatly helping me with the research along the way. I would also like to acknowledge Adriane Steinacker for inspiring me to pursue planetary astronomy, James P. Mason for proof reading and teaching me how to use macromedia Flash, Yuan Lian for providing a temperature field plot, and my parents, Paul and Lynda Shabram, my dad in particular for making me figure 9 in mathematic.

REFERENCES

Brown, Timothy M. "Transmission Spectra as a Diagnostic of Extrasolar Giant Planet Atmospheres." *The Astrophysics Journal*, no. 553 (June 2001): 1006-1026.

Chamberlain, Joseph W., and Donald M. Hunten. *Theory of Planetary Atmospheres*. Second Edition. Edited by William L. Donn. Vol. 36. San Diego, California: Academic Press, Inc. , 1987.

de Pater, Imke, and Jack J. Lissauer. *Planetary Sciences*. Cambridge: Cambridge University Press, 2001.

Fortney, J. J., K. Lodders, M. S. Marley, and R. S. Freedman. "A Unified Theory for the Atmospheres of the Hot and Very Hot Jupiters: Two classes of irradiated atmospheres." *The Astrophysical Journal*, no. 678 (May 2008): 1419-1435.

Fortney, Jonathan J. "The effect of condensates on the characterization of transiting planet atmospheres with transmission spectroscopy." *Royal Notices of the Monthly Astronomical Society*, no. 364 (2005): 649-653.

Freedman, Richard S., Mark S. Marley, and Katharina Lodders. "Line and Mean Opacities for Ultracool Dwarfs and Extrasolar Planets." *The Astrophysical Journal Supplement Series*, no. 174 (February 2008): 504-513.

Hubbard, W. B., J. J. Fortney, J. I. Lunine, A. Burrows, D. Sudarsky, and P. Pinto. "Theory of Extrasolar Giant Planet Transits." *The Astrophysical Journal*, no. 560 (October 2001): 413-4198.

Knutson, Heather A., et al. "A map of the day-night contrast of the extrasolar planet HD 189733b." *Nature*, no. 447 (May 2007): Letters.

Lecavelier des Etangs, A., F. Pont, A. Vidal-Madjar, and D. Sing. "Rayleigh scattering in the transit spectrum of HD 189733b." *Astronomy and Astrophysical manuscript* 481, no. 1 (February 2008): L83-L86.

Lodders, Katharina. "Solar System Abundances and Condensation Temperatures of the Elements." *The Astrophysical Journal* 591 (July 2003): 1220-1247.

Lodders, Katharina, and Jr., Bruce Fegley. "Chemistry of Low Mass Substellar Objects." *In press Astrophysics Update* 2 (2006): 1-30.
Marley, Mark S., Jonathan J. Fortney, Sara Seager, and Travis Barman. "Atmospheres of Extrasolar Giant Planets." *Astrophysical Journal*, 2006: 1-16.
Miller-Ricci, Eliza, Sara Seager, and Dimitar Sasselov. "The Atmospheric Signatures of Super-Earths: How to Distinguish Between Hydrogen-Rich and Hydrogen-Poor Atmospheres." *The Astrophysical Journal*, no. 690 (2009): 1056-1067.
Pont, F., H. Knutson, R. L. Gilliland, C. Moutou, and D. Charbonneau. "Detection of atmospheric haze on an extrasolar planet: The 0.55 - 1.05 micron transmission spectrum of HD189733b with the Hubble Space Telescope." *MNRAS*, 2007: 1-11.
Seager, S., and D. D. Sasselov. "Theoretical Transmission Spectra During Extrasolar Giant Planet Transits." *The Astrophysical Jouranl*, July 2000: 916-921.
Showman, Adam P., Curtis S. Cooper, Jonathan J. Fortney, and Mark S. Marley. "Atmospheric Circulation of Hot Jupiters: Three-Dimensional Circulation Models of HD209458b with Simlified Forcing." *Astrophysical Journal*, no. 682 (2008): 559-576.
Showman, Adam P., et al. "Atmospheric Circulation of Hot Jupitors: Coupled Radiative-Dynamical General Circulation Model Simulations of HD 189733b and HD20458b." *The Astrophysical Journal*, 2007: 1-18.
Sing, David K., A. Vidal-Madjar, A. Lecavelier Des Etangs, J. -M. Desert, G. Ballester, and D. Ehrenreich. "Determining Atmospheric Conditions at the Terminator of the Hot-Jupiter HD209458b." *Astrophysical Journal*, no. 686 (2008): 667-673.
Spiegel, David S., Zoltan Haiman, and B. Scott Gaudi. "On Constraining a Transiting Exoplanets Rotation Rate with its Transit Spectrum." *The Astrophysical Journal*, no. 669 (November 2007): 1324-1335.

GLOSSARY

Absorption spectrum: Generally, in astrophysics, one sees absorption lines when atoms/molecules absorb photons at a particular frequency from a beam of broad-band radiation…the intensity at the center of the line is less than the intensity of the background continuum level (de Pater and Lissauer 2001, section 4.3.1). A line represents a small portion of the spectrum, where a band refers to a large portion of the spectrum.

Chemical abundances: The abundance of a certain chemical or molecule is determined by how much of that molecule is present compared to the other molecules that are present in a composition. The atomic abundances for CI chondrites are usually in terms of atoms/10^6Si (de Pater and Lissauer 2001).

Chemical mixing ratios: The mixing ratio is often indicated as a percentage or a ratio of the particular species with respect to the total number of particles in a given volume, usually given in parts per million (ppm) (de Pater and Lissauer 2001, section 4.3.3). Chemical mixing ratios are used to quantify atmospheric composition.

Extrasolar planet: An extrasolar planet is a planet found outside of our solar system.

Hot Jupiter: A large gas giant, on the order of a Jupiter mass, close to its parent star and therefore very hot, usually tidally locked.

Hydrostatic equilibrium: Assumes a fluid body where the gravitational force and the pressure gradient of the planet are balanced. This is represented by $dP/dz = -\rho g$, where P is pressure, ρ is density, g is gravity, and z is the height in the atmosphere.

Light curve: A measure of a star's intensity with time as planet passes in front of it with the same orbital inclination as Earth (see Fig. 20).

Limb (planetary limb): When gas giants in our solar system pass in front of the sun, the limb of the planet is usually defined as either the height in the atmosphere where the cloud tops are, or the 1 bar pressure level. The atmosphere above the limb is called the transparent atmosphere, although the transparent atmosphere can be optically thick for some wavelengths (Seager and Sasselov 2000).

CI chondrites: These are a class of primitive meteorites that have not melted and are composed of material condensed directly from the solar nebula and surviving interstellar grains (de Pater and Lissauer 2001, section 8.1).

Normal optical depth: The optical depth of a planetary atmosphere calculated for a propagation direction that is normal to the planet.

Opacity: Opacity is a term used to describe how well light can pass through a medium. When a wavelength of light passes through a medium, it is absorbed, scattered, or unperturbed.

Rayleigh scattering: Rayleigh scattering is when light is scattered off small particles that are much smaller than the wavelength of light being scattered. This is common in the upper atmosphere of gas giants (de Pater and Lissauer 2001).

Scale Height: The scale height is determined by $H = RT/\mu g$, where R is the gas constant, T is the temperature, μ is the molar mass of atmosphere, and g is the planet's gravity. The scale height assumes hydrostatic equilibrium and represents the height in the atmosphere at which the pressure is reduced by a factor of $1/e$.

Slant optical depth: The optical depth of a planetary atmosphere calculated for a propagation direction that is tangential to the planet.

Solar abundances: Chemical abundances of the sun's photosphere. Solar abundances are very similar to meteoritic CI chondrite abundances. (de Pater and Lissauer 2001, section 8.1).

Terminator: Great circle the separates the day-night hemispheres.

Tidally Locked: As a result of tidal dissipation, the rotation of a body is slowed, eventually becoming tidally locked, meaning that the body rotates only once for every time it completes an orbit. This produces a planet that has one face always pointed at the star and one face always pointed away.

Transit: A transit is when a planet passes in front of its parent star within the same orbital inclination of Earth so that we can see a spectral imprint of the planet on the star.

Transmission spectra: the height in the planets atmosphere at which it first becomes opaque to tangential rays as a function of wavelength (Brown 2001). In other words, it is the effective planet radius as a function of wavelength.

APPENDIX

A: Detection methods: radial velocity detection technique

The radial velocity detection method is concerned with observing a star, and determining whether or not that star has a wobble. If it does, the wobble would be a result of the star and another body orbiting each other. An orbiting planet is in reality orbiting around the center of mass of the star-planet system, and the star is as well orbiting this center of mass point. We detect the stars motion by observing a Doppler shift in the stars light. As the star is approaching, the light is blue shifted, or stacked against itself so the wavelength appears compressed. As it winds around its orbit and is going away from us, we see the wavelengths of light from the star become stretched (see Fig. 18). From Earth, an observer sees only a line-of-sight component of the stars motion, as the system orbits. The velocity of the star can be obtained and plotted with time and hence a radial velocity curve (see Fig. 19).

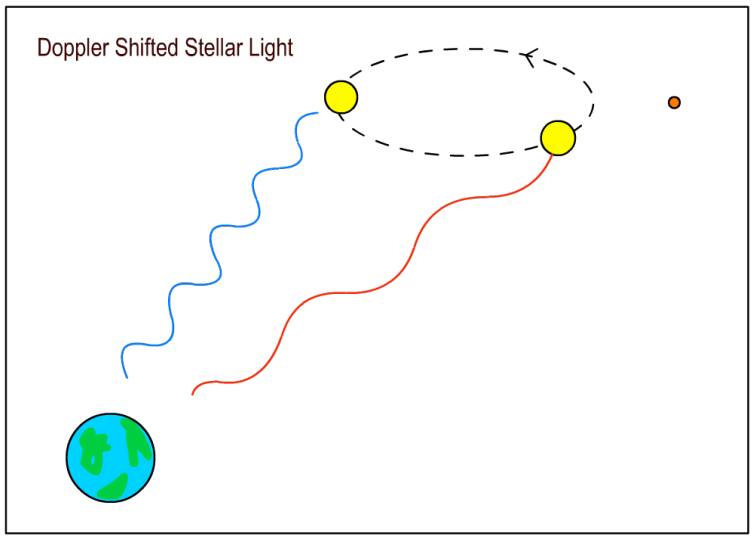

Figure 18. Parent star's light is Doppler shifted. The star and planet orbit a center of mass point, and the motion of the star around this point is seen as a Doppler shift.

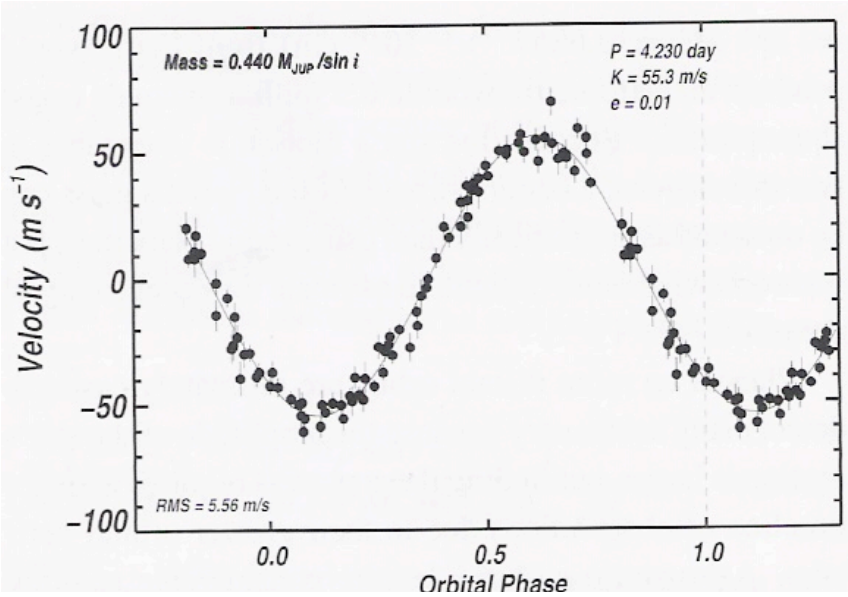

Figure 19. Radial velocity plot. The star's velocity changes with its orbital phase (de Pater and Lissauer 2001).

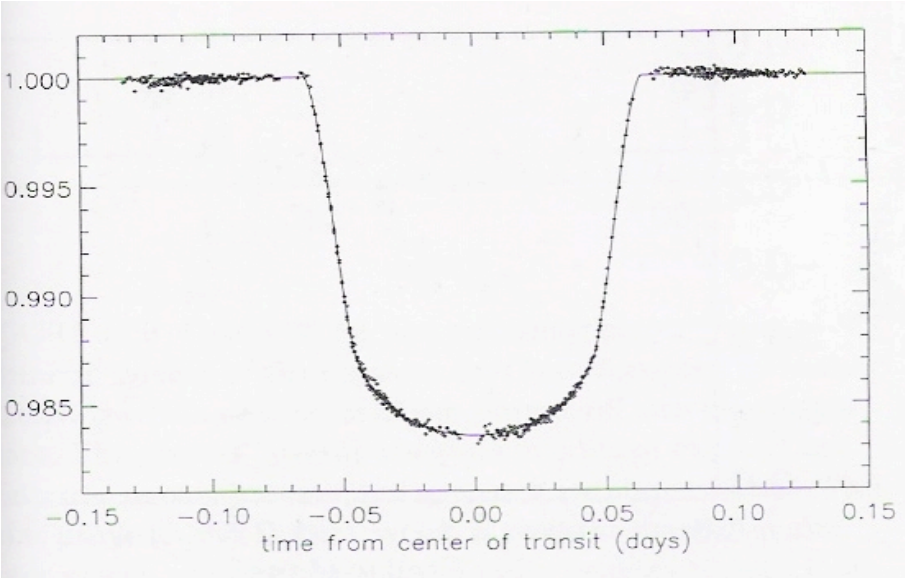

Figure 20. Light curve for HD209458b. This is an example light curve, the stars intensity with time and a planet passes in front of it (de Pater and Lissauer 2001).

After a star-planet system has been detected via the radial velocity method, observations of the stars intensity with time can determine whether or not the planet is transiting its parent star. A plot of the star's intensity with time is called a light curve (see Fig. 20)

B: Radial velocity equation and explanation

An equation for the maximum radial velocity of a planet orbiting a star is

$$K = \left(\frac{2\pi G}{P_{orb}}\right)^{1/3} \frac{M_p \sin i}{\left(M_* + M_P\right)^{2/3}} \frac{1}{\sqrt{1-e^2}}, \tag{7}$$

where K is the maximum radial velocity or the amplitude of the radial velocity curve (see Fig. 17), $\boldsymbol{M_p}$ is the mass of the planet, $\boldsymbol{M_*}$ is the stellar mass, P_{orb} is the orbital period, $\boldsymbol{e}$ is the eccentricity of the orbit, and $\boldsymbol{G}$ is the gravitation constant (de Pater and Lissauer 2001). This radial velocity equation is used to constrain the planetary mass. When a planet is detected by the radial velocity method we know that its inclination must have a component in the same orbital plane as Earth (see Appendix A). Right away we know

that this planet is a transiting planet candidate. If the planet transits is parent star, the orbital inclination can be determined and from this the Mass of the planet. If the planet does not transit there is a large uncertainty in the planets mass. This is because the radial velocity tells us what $M_p \sin i$ is, and we need to know $\sin i$ in order to deduce the planet's mass.

C: Computer model

Fortran 77 is used to model transmission spectra. Below (see Fig. 21) is a snippet of code that performs the 2D slant optical depth calculation. In this code, zkfac(j) is the slant optical depth in the atmosphere at a altitude r(j) (km) or rr(j) (cm). tau(i) is the molecular cross section for a horizontal distance Δs, in the code this is represented as dl, and znum(i) is the particle density for this same distance Δs.

```
524
525 c-------------------------------------------------------------------------------
526         do 300 j = 1,npts-1
527
528         length=1.0d5*dsqrt((r(1)**2)-((rsurf/100000.d0)**2))
529         dl=length/npts            !calculate length of each box
530
531
532            do 200 i=j,1,-1
533            rr(j)= r(j)*1.0d5                        !radial height in atmosphere
534            hzntl(i) = dl*i                          !horizontal position along strip
535            angle = (DATAN(hzntl(i)/rR(j)))*radians  !angular position of box
536
537            if(angle.LT.(abs(ph)-2.8125d0).OR.angle.GT.(abs(ph)+2.8125d0)) then
538            zkfacnow(j) = 0.d0                  !If the box is outside the angular region,
539                                                !fill in zero for that box
540            else
541            zkfacnow(j)= tau(i)*znum(i)*dl      !If box is inside angular region, do the
542                                                !slant optical depth calc.
543
544            zkfac(j) = zkfac(j) + zkfacnow(j)   !Sum all boxes in each altitude to get
545                                                !total slant opt. depth at that altitude.
546            end if
547
548 200        continue
549 300    continue
550 c-------------------------------------------------------------------------------
```

Figure 21. Section of computer model that performs 2D slant optical depth calculation. This part of the code uses multiple P-T profiles specific to the location in the atmosphere to calculate the slant optical depth through a slice of atmosphere.

D: 2D Transmission Spectra

Presented below are 2D transmission spectra for 8 different longitude strips: -180^0, -135^0, -90^0, -45^0, 0^0, 45^0, 90^0, and 135^0, modeled for HD189733b. These same longitude strips are overlaid on each other to produce an effective 3D model (see Fig. 14). The negative longitude values represent the west side of the planet, where the positive values represent the east side. Due to the hot spot of the substellar point being shift eastward around the equator, we see hotter transmission spectral features for all the positive longitude values (east).

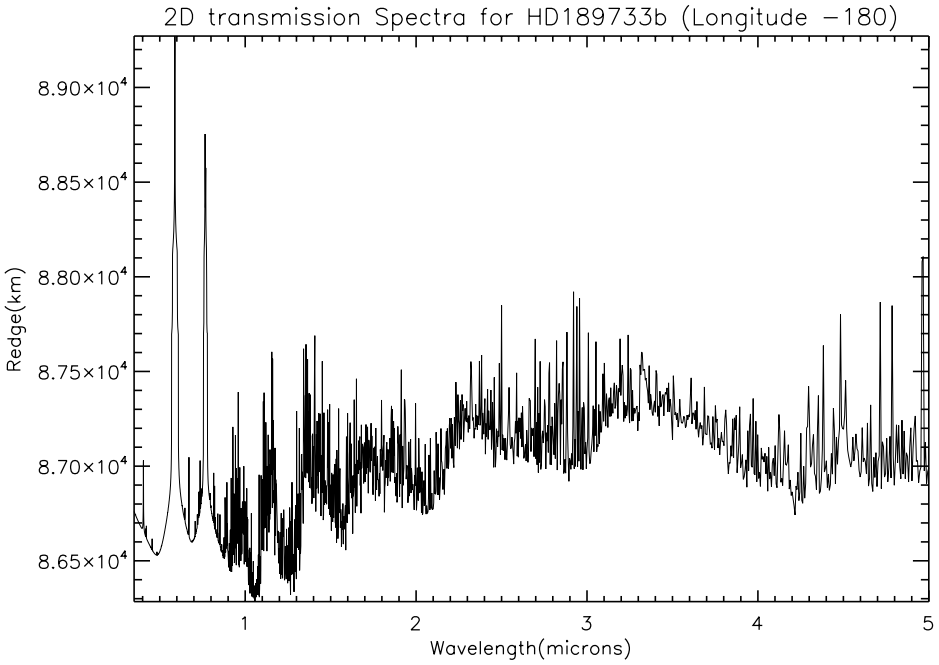

Figure 22. 2D transmission spectra for colder region of atmosphere away from equatorial jet, passing over the real north pole of planet.

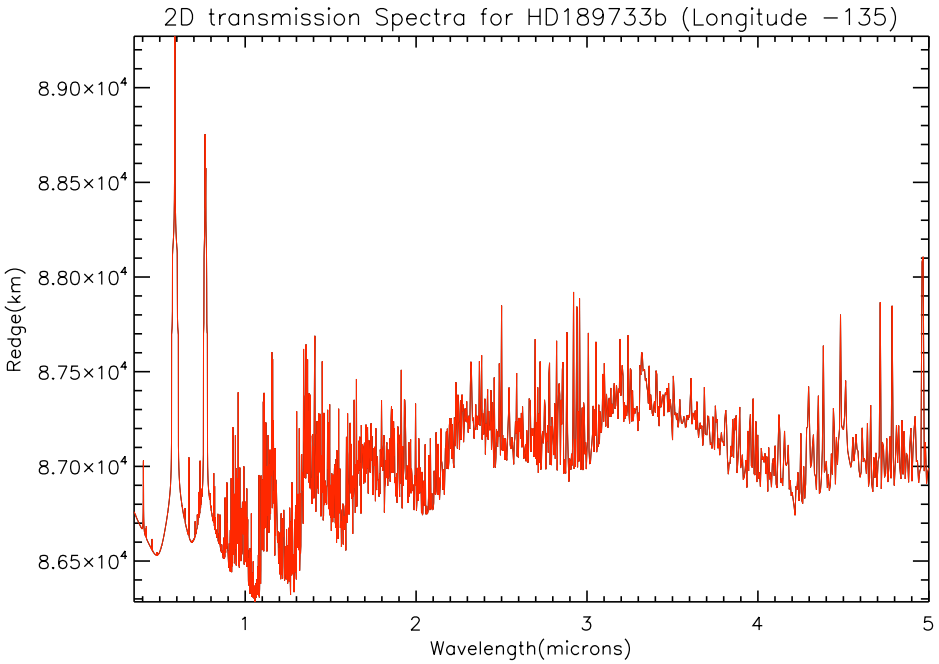

Figure 23. 2D transmission spectra for colder west side region of planet.

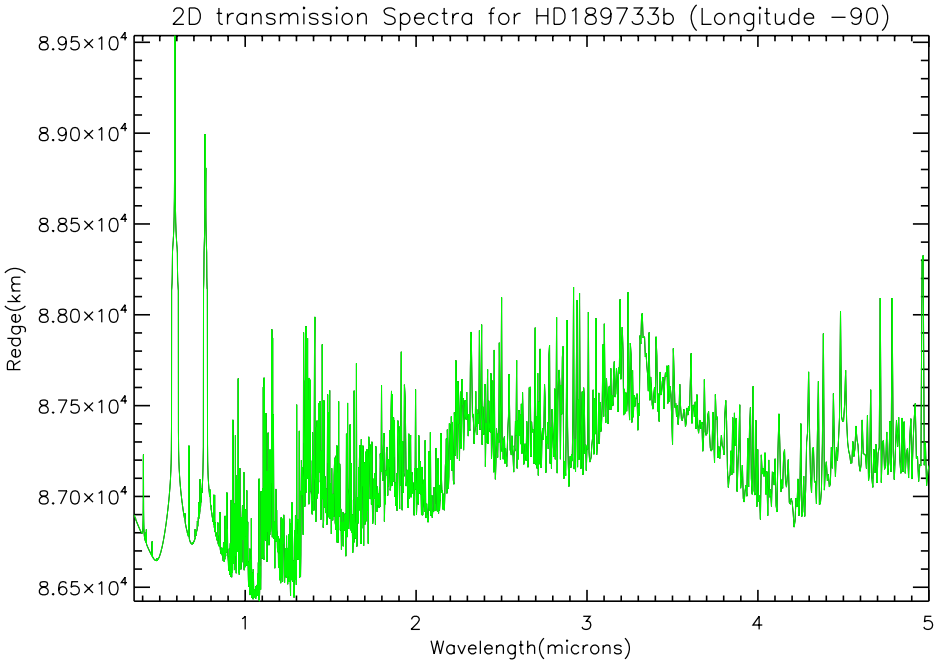

Figure 24. 2D transmission spectra for hotter region of planet in equatorial jet. The hot spot of the planet is shifted downwind eastward of the actual substellar point. This is a plot of the west side of the equator, which in comparison to the east side of the equator looks cooler.

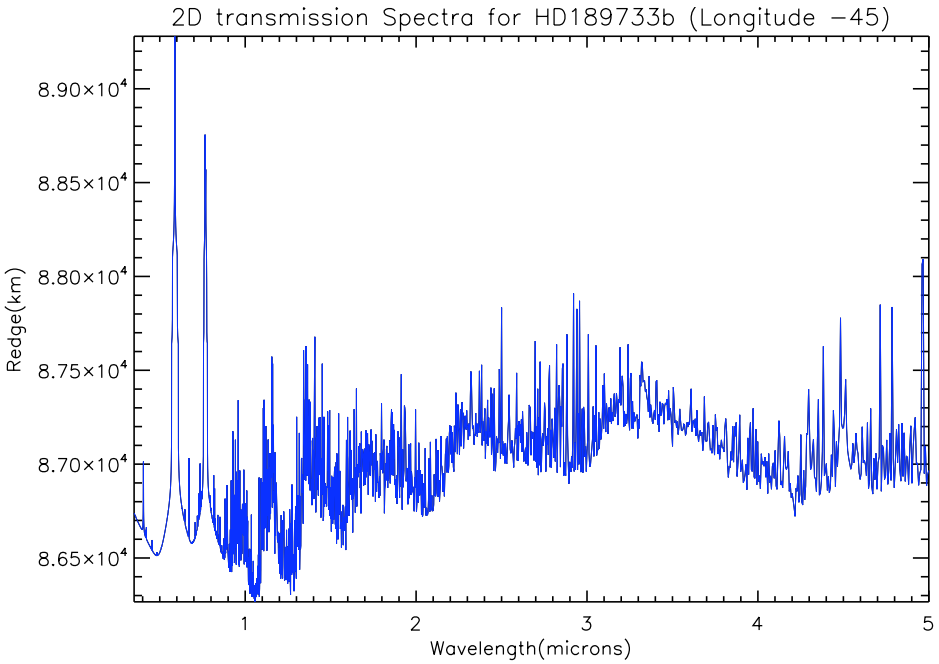

Figure 25. 2D transmission spectra outside equatorial jet on the colder west side region of the planet.

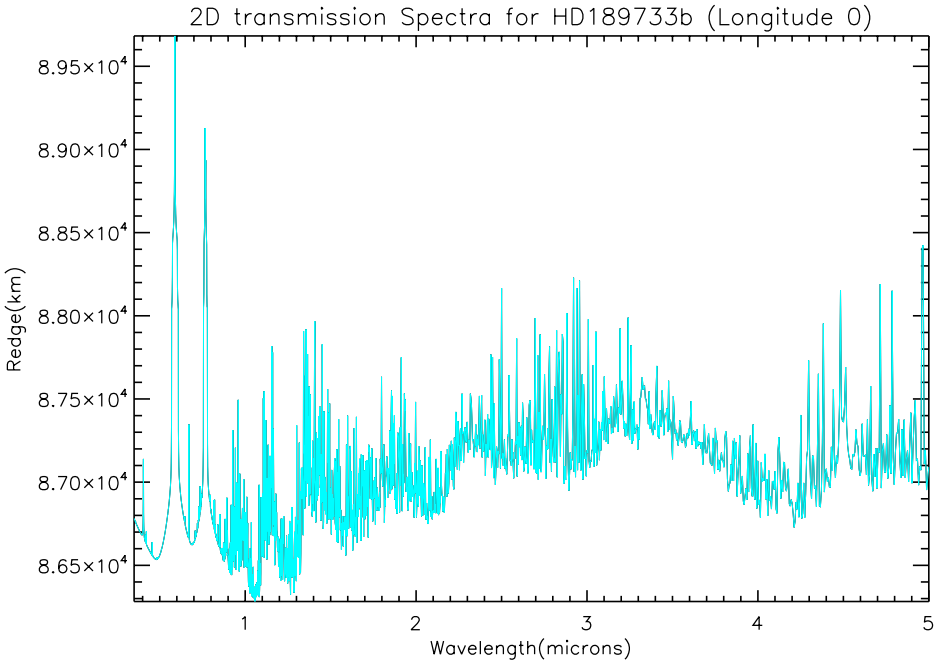

Figure 26. 2D transmission spectra for colder region of planet.

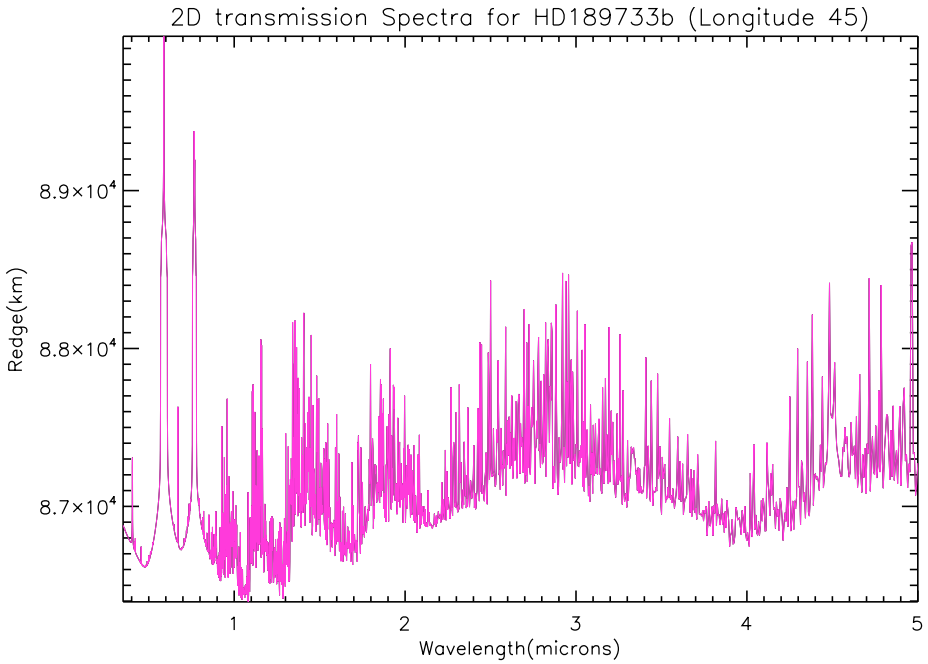

Figure 27. 2D transmission spectra for the hotter east side region of planet, outside equatorial jet.

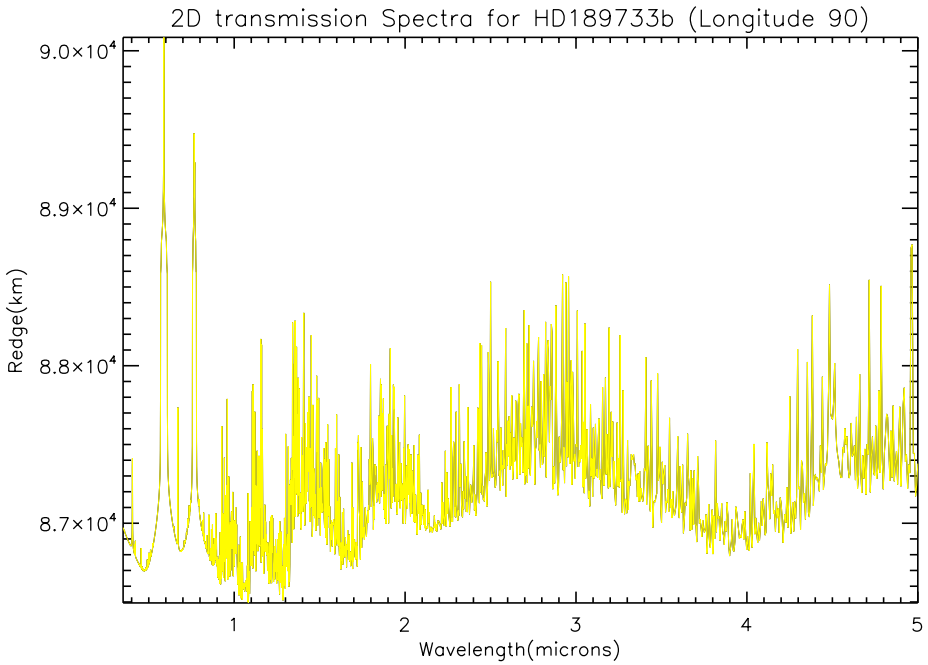

Figure 28. 2D transmission spectra for hotter region of planet in the equatorial jet. Here, the transmission spectrum through the east side of the equator is presented. The hot spot has been shifted east along this side of the equator producing hotter transmission spectra.

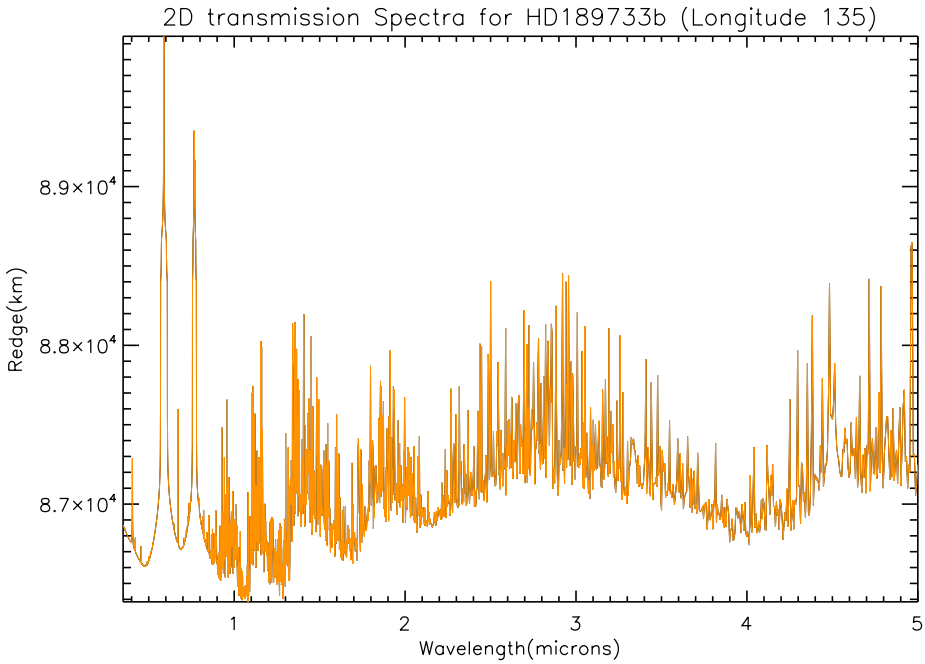

Figure 29. 2D transmission spectra for hotter east side region of planet outside equatorial jet.

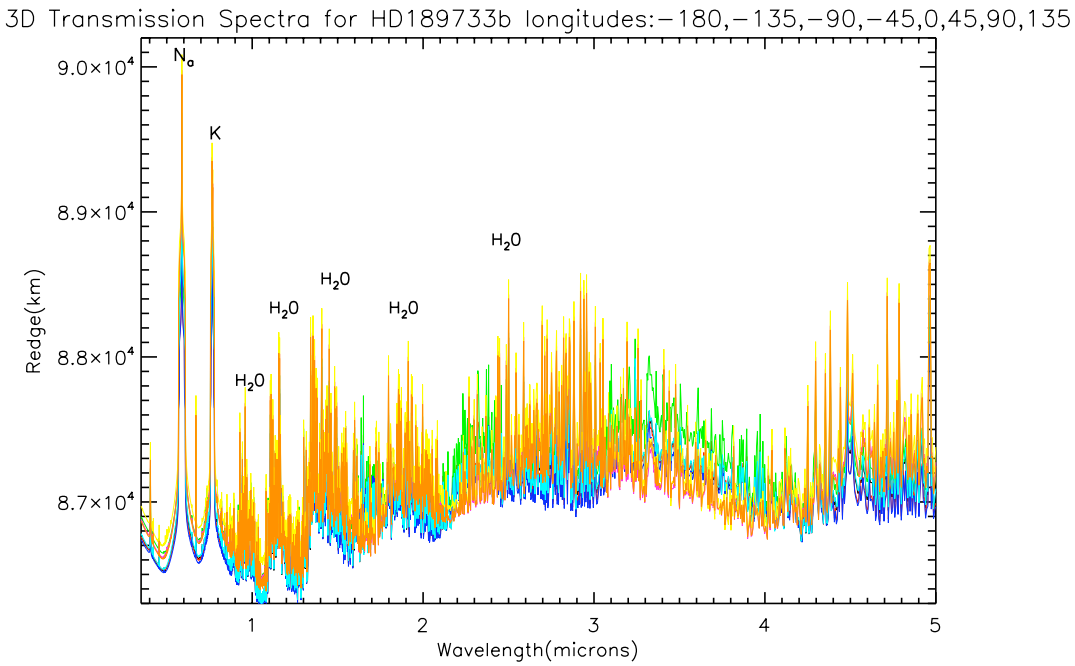

Figure 30. Plot of overlaid transmission spectra for 8 longitude strips shown in figures 22-29. This plot shows how the curves differ from each other. Figure 15 is an average of these 8 transmission spectra.